No. AD 85

XIX
IAF

THE SIMULATION OF LUNAR TRAJECTORIES WITH ASSOCIATED SENSITIVITY AND MIDCOURSE CORRECTION VELOCITY STUDY

by

WALKER H. LAND, JR.
Staff Engineer
International Business Machines Corporation
Federal Systems Division
Space Systems Center
Huntsville, Alabama, U.S.A.

IAF Paper
AD 85

19th Congress of the International Astronautical Federation

NEW YORK, N. Y./OCTOBER 13-19, 1968

First publication rights reserved by International Astronautical Federation, 250, rue Saint Jacques, Paris 5, France. (Price: U. S. $1.00)

Additional copies of this preprint may be obtained at American Institute of Aeronautics and Astronautics (Special Publications Department - IAF), 1290 Avenue of the Americas, New York, N. Y. 10019, U.S.A.

THE SIMULATION OF LUNAR TRAJECTORIES WITH ASSOCIATED SENSITIVITY AND MIDCOURSE CORRECTION VELOCITY STUDY

Walker H. Land, Jr., Staff Engineer
International Business Machines Corporation
Federal Systems Division
Space Systems Center
Huntsville, Alabama

Abstract

This paper (1) describes the mission profile from liftoff to re-entry of free-return circumlunar trajectory and (2) discusses an associated sensitivity and midcourse correction study. Sensitivity and midcourse analyses showed that the effects of the moon are small at the eight-hour midcourse correction point and that the N-body model may be replaced with a two-body model in computing the midcourse correction velocities at the eight-hour point unless exacting accuracy is required. (3) The midcourse velocity components in a given direction due to position and velocity errors, taken separately, yield the same result as when these errors are taken together and (4) the magnitude of midcourse correction velocity is linearly related to individual errors in in-plane and out-of-plane cutoff flight path angles, cutoff radius and velocity magnitude, and cutoff out-of-plane position dispersions. (5) Out-of-plane position and flight path angle errors require less midcourse correction than do in-plane position magnitude error or flight path angle error.

I. Introduction

The purposes of this paper are to describe (1) the mission profile from liftoff to re-entry of a free-return circumlunar trajectory and (2) an associated sensitivity and midcourse correction velocity study. The discussion contains (a) the description of selected properties of the midcourse correction velocity magnitude and velocity components, (b) the relationship of the midcourse correction velocity to the perturbations in the geocentric translunar injection components, (c) the effect of simplifying the N-body math model on the midcourse correction velocity, and (d) the midcourse correction velocity magnitude as a function of errors in the in-plane and out-of-plane velocity angle errors, velocity magnitude, radial magnitude, and out-of-plane position dispersions. The paper begins with the description of the mission that was utilized in the sensitivity and midcourse correction velocity study.

II. Description of Mission Profile

The purpose of this section is to describe the mission profile[1] from liftoff to re-entry. The profile was obtained by simulation using a six-dimensional trajectory generator (6D) for the ascent-to-orbit,[2] parking orbit, and translunar injection phases. The guidance scheme utilized is the iterative guidance mode with the targeting conditions for the translunar injection burn being provided by the hypersurface. The translunar and transearth legs were generated using an N-body lunar iterative program which is discussed in the translunar and transearth subsection.

Ascent-to-Orbit Trajectory

The launch profile of the Saturn V consists of burning the S-IC and S-II stages to depletion, followed by suborbital ignition and burn of the S-IVB stage to insert the vehicle into an earth parking orbit. Launch is to occur on September 17, 1969, from the Merritt Island launch area at the Kennedy Space Center with a launch azimuth 90° east of north and a launch time of 11 hours, 35 minutes, and 12.50 seconds G.M.T. with launch coordinates 28.64° north geodetic latitude and 80.63° west longitude. The S-IC flight consists of vertical liftoff and flight for the first 12 seconds. An initial roll maneuver will be commanded, and a programmed tilt, initiated and followed until tilt arrest at 145 seconds into the flight, after which time χ_p will be frozen until iterative guidance mode (IGM) initiation during S-II flight. Cutoff of the S-IC inboard engine occurs at 155.20 seconds after liftoff, and the four outboard engines will be cut off 4.04 seconds later. S-IC cutoff is followed by a 3.80-second coast period which will simulate the F-1 engine thrust decay, S-IC/S-II separation, and J-2 engine thrust buildup. The F-1 engine decay to 10-percent thrust occurs in approximately 0.55 seconds, after which time the ullage and retro-rockets will be fired. The remainder of this coast is consumed by separation and by J-2 thrust buildup.

At 163.040 seconds after liftoff, the J-2 engines of the S-II stage reach full thrust; and at 197.360 seconds, the IGM is initiated and used until parking orbit insertion. During S-II stage flight, the LH_2/LOX mixture ratio is changed, which results in an 82.6086 percent value of the original of S-II stage thrust. This EMR shift occurs at 442.5 seconds after liftoff. At 191.360 seconds after liftoff, the S-IC/S-II interstage is jettisoned. Cutoff of the five S-II stage J-2 engines occurs simultaneously 536.24 seconds after launch.

The S-IVB stage immediately ignites (536.24 seconds) and follows IGM until parking orbit insertion at an altitude of 185.198 km into a nearly circular parking orbit. Insertion time is 681.639 seconds after liftoff with a vehicle weight of 132,752.160 kg. The geometry of the ascent phase is depicted in Figures 1a and 1b and the altitude and inertial velocity during the boost-to-parking-orbit is shown in Figure 2.

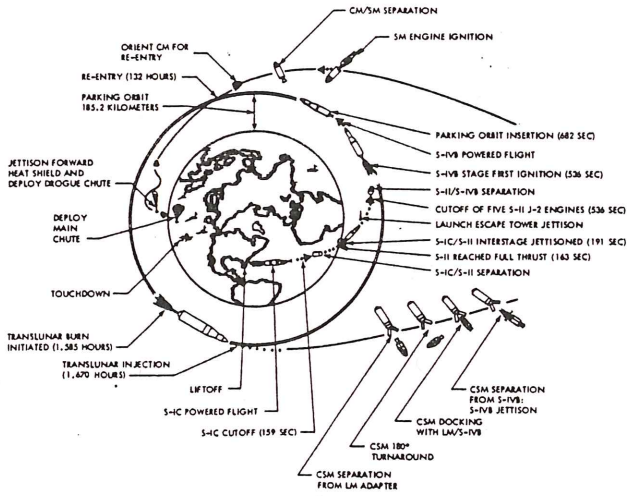

Figure 1a. Mission Profile (Not to Scale)

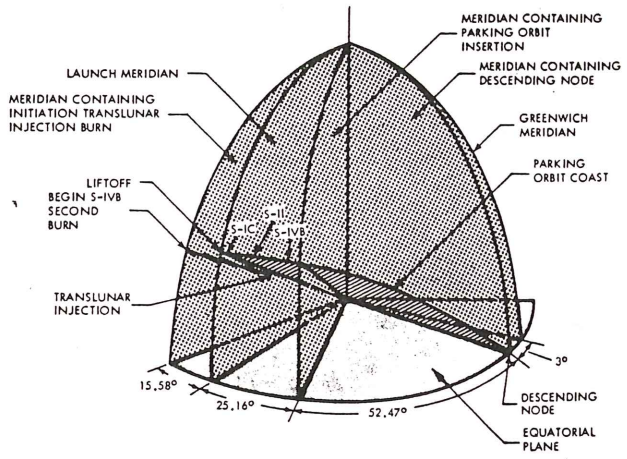

Figure 1b. Geometry of Ascent Phase, Parking Orbit Phase, and Translunar Injection Phase

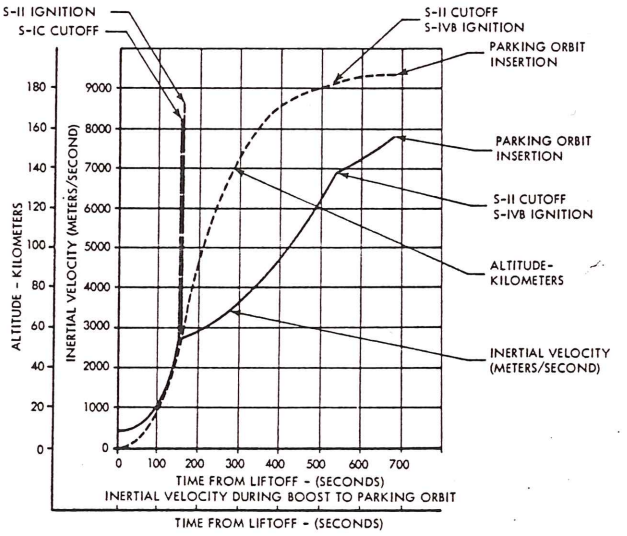

Figure 2. Altitude During Boost to Parking Orbit

Earth Parking Orbit Phase

Parking orbit insertion occurs at 25.76° north geodetic latitude and 55.47° west longitude. The parking orbit coast time is 1.3958 hours. All venting and ullage thrusting is assumed to act collinearly with the velocity vector so as to increase the space vehicle energy. Figure 3 shows the variation in inertial velocity and altitude during parking orbit coast. Figures 1a and 1b show the relationship of the parking orbit phase to the ascent-to-orbit and translunar injection phases. Note that the descending node occurs at 3° west longitude.

Translunar Injection Phase

The translunar injection burn is initiated 1.5855 hours after liftoff at 28.22° north geodetic latitude and 96.22° west longitude (Figure 1b). The optimum burn time is 342.264 seconds with translunar injection occuring at 23.21° north geodetic latitude and 68.06° west longitude (Figure 1b) with an azimuth heading of 107.21° east of north. Figure 4 shows the inertial velocity as a function of time during translunar injection burn, while Figure 5 depicts the inertial flight path angle and altitude during this burn. Note that the

inertial velocity increases from 7,896.9 meters/sec at the beginning of the burn to 10,869.015 meters/sec at translunar injection, while the altitude and the flight path angle increase from 188.088 km and 0^{o} to 297.711 km (or 6,672.596 km with respect to the earth center) and 6.32^{o} respectively. The guidance scheme utilized in the translunar injection phase is the iterative guidance mode with the targeting parameters supplied to IGM by the hypersurface. The hypersurface concept will be discussed in Section III.

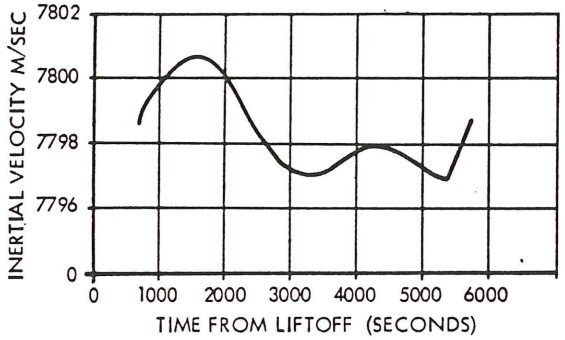

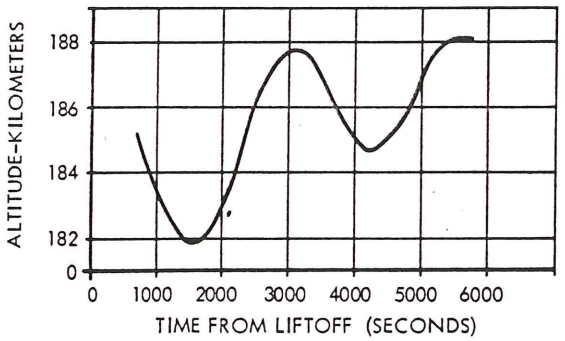

Figure 3. Inertial Velocity and Altitude During Parking Orbit

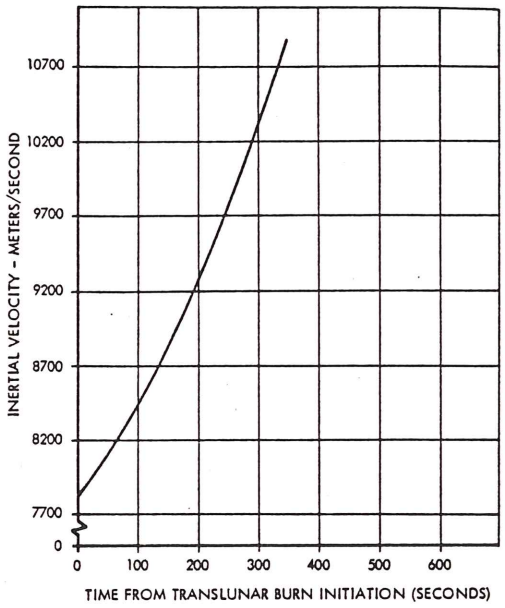

Figure 4. Inertial Velocity During Boost to Translunar Injection

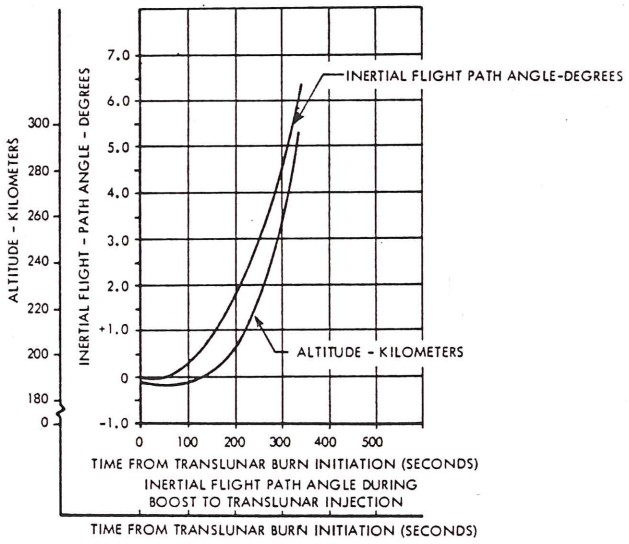

Figure 5. Altitude and Flight Path Angle During Boost to Translunar Injection

Translunar and Transearth Legs

Figure 6 depicts the translunar and transearth legs and the relationship of this portion of the mission to the ascent-to-orbit, parking orbit, and translunar injection phases. The translunar and transearth legs are generated by a numerical integration program developed by several IBM facilities.[3] Forces and trajectory integration are computed in a rectangular coordinate system which is referenced to the mean vernal equinox of date. Description of the vehicle state is also executed in the earth-moon coordinate system, which is defined by the position and velocity of the moon at perilune time of the symmetrical trajectory. The origin of the coordinate systems is the center of the earth when the vehicle is in the vicinity of the earth and automatically switches from the earth reference to the moon reference (on the translunar leg) at a radius of nine earth radii (lunar sphere of influence) from the center of the moon. On the transearth leg the program again switches from the selenocentric (moon centered) to the geocentric frame at the lunar sphere of influence. Ephemeris tape used by the

program is an edited version of the U.S. Naval Observatory Data Tape, which contains data for the sun, moon with moon libration matrices, Venus, Mars, and Jupiter. The trajectory program also includes the effect of the second, third, and fourth earth harmonics, and also has the option of the simulation of a patched conic model to a complete N-body model as described above. Effects of each or all the earth harmonics may be incorporated to any desired distance out to and past the lunar sphere of influence; whereas, the effect of moon triaxiality may be computed to any desired distance from the moon out to and past the lunar sphere of influence. The program also computes in single precision with double precision accumulation and straight double precision. Integration of the equations of motion is executed by the Cowell Method. The Cowell Method means here that the equations of motion are integrated directly in rectangular coordinates by an eighth-order central difference process where higher ordered differences are expressed in terms of tabular values. A modified Runge-Kutta starter routine is used, and the program computes either in fixed or variable step sizes. This starter routine is also used each time the step size is altered. Position units used are kilometers and earth-radii; velocity units used are meters/second and earth-radii/hour; angular units used are degrees and radians; the basic unit of time is the hour. The program first generates the transearth leg from perilune (the distance of closest approach of the vehicle to the moon) to re-entry by an iterative process on the boundary conditions at these points and then generates the translunar leg from perilune to translunar injection, such that not only the translunar injection conditions are satisfied, but also the perilune conditions (obtained on the transearth leg) are not violated.

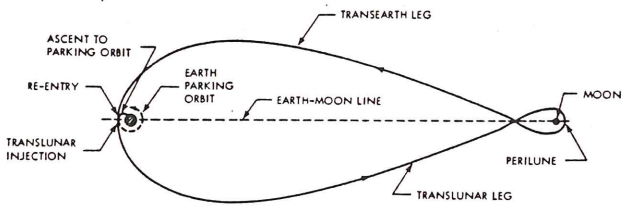

Figure 6. Planar Geometry of Ascent Phase, Parking Orbit Phase, Translunar Injection Phase, Translunar and Transearth Phases

Translunar injection occurs 1.670 hours after liftoff while the translunar injection to perilune time is 61.7243 hours. The perilune time, therefore, occurs 63.4087 hours after liftoff. The vehicle velocity magnitude at perilune is 2,603.82 meters/second with a flight path angle of 90^{o}. The perilune to re-entry time is 68.6256 hours with re-entry boundary conditions occurring 132.0343 hours after liftoff. The re-entry (radius and velocity) magnitudes are 6,430.700 kilometers and 11,061.949 meters/second with an associated flight path angle of 90^{o}.

Table 2-1 depicts the time-event sequence from liftoff to re-entry.

III. Sensitivity and Midcourse Correction Velocity Analysis

The primary purpose of this section is to describe the relationship of midcourse correction velocities to errors at translunar injection. Specifically contained in this section are: (a) the description of certain properties of the midcourse correction velocity magnitude and velocity components, (b) the relationship of the midcourse correction velocity to the perturbations in the geocentric translunar injection components, and (c) the effect of simplifying the N-body math model on the midcourse correction velocity. The midcourse correction velocity magnitude as a function of errors in the in-plane and out-of-plane velocity angle errors, velocity magnitude, radial magnitude, and out-of-plane position deviation are described. The first subsection outlines the simulation (program) sequence required to accomplish these studies, while the last sections contain the analysis outlined above and the results of these analyses.

Program Sequence

The purpose of this subsection is to outline the program sequence necessary to make the midcourse corrections required to compensate for errors at translunar injection. In this discussion it is assumed that the nominal and perturbed translunar injection states have been obtained using the simplified hypersurface, 6D and IBM programs. That is, the nominal trajectory state at translunar injection (as discussed in Section II) and perturbed states from this nominal translunar injection state are available.

Table 2-1

TIME-EVENT SEQUENCE

Time From Liftoff	Event	Comment
0	Liftoff	
155.20 sec	Cutoff of S-IC InBoard Engine	Vertical Liftoff, No Roll and Vertical Flight for First 12 Seconds
159.24 sec	OutBoard Engines Cutoff	
163.040 sec	J-2 Engines Reached Full Thrust	The 3.80 sec Coast Period used to Simulate F-1 Engine Decay, S-IC/S - II Separation and J-2 Engine Thrust Buildup
191.360 sec	S-IC/S-II Interstage Jettisoned	
197.360 sec	IGM Initiated and used until Parking Orbit Insertion	
442.58 sec	EMR Change	
536.244 sec	Cutoff of Five S-II Stage J-2 Engines Occurred Simultaneously and S-IVB Stage Ignition	
681.639 sec	Parking Orbit Insertion	Occurs at 25.76° North Geodetic Latitude and 55.47° West Longitude
1.585 hours	Translunar Injection Burn Initiated	Initiated at 28.22° North Geodetic Latitude and 96.22° West Longitude
1.670 hours	Translunar Injection	Injection occurs at 23.21° North Geodetic Latitude and 68.06° West Longitude. Optimum Burn Time of 342.264 sec. Injection Parameters, Inertial Velocity and Flight Path Angle of 10,869.015 m/s and 6.32° and Altitude of 297.71 KM.
63.408 hours	Perilune Reached	Vehicle Perilune Velocity is 2,603.802 m/s. Flight Path Angle of 90° and Altitude of 103.71 KM (56 NM).
132.034 hours	Re-Entry	Boundary Conditions are: Re-Entry Radius of 6,430.700 KM; Re-Entry Velocity Magnitude and Flight Path Angle of 11,061.949 m/s and 90°.

The nominal lunar trajectory state from translunar injection to the eight-hour midcourse correction state is obtained from either the trajectory tape of the translunar leg generated in Section II or by the lunar trajectories program. (The lunar trajectories program generates the trajectory from the nominal translunar injection state to the eight-hour midcourse correction point. The program contains the same math model and options as the lunar iterative program with the exception of the perilune iterative procedure.) The first order perturbations from this nominal trajectory are obtained using the sensitivity matrix. This matrix is computed from the gravity gradients which are evaluated using the position vector components of the nominal trajectory (see Appendix B). The sensitivity matrix at the midcourse correction state is employed in the midcourse program to compute the velocity correction required to compensate for the error at translunar injection, so that the perturbed trajectory will enter the lunar sphere of influence with the nominal position at the nominal time. A more detailed description and required analytical development of these programs, in addition to the hypersurface program description is contained in the following subsection.

Simulation Programs

Lunar Trajectories Program The lunar trajectories program may be used to obtain any portion or all of the translunar leg (from translunar injection to perilune) or the transearth leg (from perilune to re-entry). Among others, the description of the force computations and the numerical integration procedure employed are contained in Section II.

Sensitivities Program The sensitivities program involves calculating and integrating gravity gradients which are evaluated using the position vectors of the nominal trajectory from translunar injection to midcourse. These computations yield values of the sensitivity matrix at selected points along the nominal trajectory from translunar injection to the midcourse correction point. Appendix B and a reference [4] contain the basic analytical development of the sensitivities matrix and the sensitivity integration program. The program used in this analysis contains a fixed (rather than a variable) integration step size and employs a fifth-order interpolation scheme between these fixed step sizes to improve accuracy. The resulting sensitivity matrices are also updated by matrix multiplication every thirty integration steps to improve the accuracy in computation of these sensitivity matrices.

Midcourse Correction Program The midcourse correction program uses the results of the sensitivities program to compute the midcourse velocity required to compensate for errors at translunar injection (such that the perturbed trajectory will enter the lunar sphere of influence at a given position and time) as follows:

(1) Find the aim point on the lunar sphere of influence. The aim point is determined by passing the Kepler arc (elliptic arc)[5] from the nominal midcourse state and iterating until the lunar sphere of influence is found. This position (on the lunar sphere of influence) is recorded as the aim point. The trajectory from this nominal eight-hour point to the lunar sphere of influence is depicted as the nominal translunar leg of Figure 7.

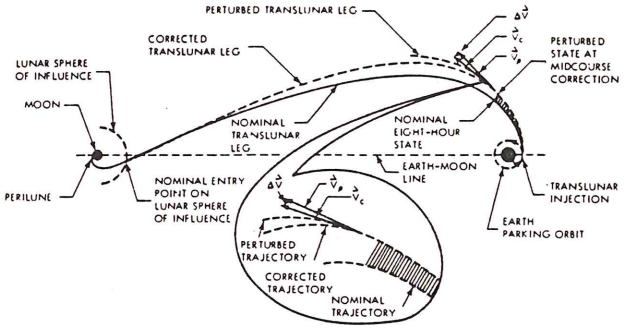

Figure 7. Geometry of Midcourse Correction Velocity Method (Not to Scale)

(2) Multiply the error at translunar injection due to in-flight perturbations by the linear sensitivities matrix, evaluated at the midcourse correction state, to obtain the effect of this error at the midcourse correction state. The linear sensitivities will yield the perturbed trajectory depicted in Figure 7, as measured from the nominal trajectory from translunar injection to the eight-hour midcourse correction point.

(3) Add this perturbed state ($\Delta\vec{R}$ and $\Delta\vec{V}$) to the nominal state ($\vec{V}_n$, $\vec{R}_n$) at the eight-hour point on the nominal trajectory to obtain the vehicle state ($\vec{R}_p$, $\vec{V}_p$) along the perturbed trajectory. This addition yields the effect (at midcourse) due to the error at translunar injection.

(4) Use the Lambert Theorem-Kepler Arc program to find the Kepler arc between the perturbed state at midcourse and the aim point on the lunar sphere of influence. This Kepler arc will allow the perturbed trajectory, which becomes the corrected translunar leg of Figure 7 at the midcourse correction point, to pass through the nominal position on the lunar sphere of influence at the nominal time by providing a velocity correction at the midcourse correction state. See Lambert's Theorem.[6]

(5) From Figure 7 it may be seen that the vector velocity correction (velocity impulse) which must be applied to the vehicle is the vector difference of the Lambert velocity ($\vec{V}c$) and the vehicle velocity along the perturbed trajectory ($\vec{V}p$).

The analysis outlined in the above five steps is performed in the geocentric equatorial coordinate system and several studies (described subsequently) are conducted in this coordinate system. In the geocentric equatorial coordinate system, the nominal and perturbed translunar injection states are given in terms of the components of the position and velocity vectors at the cutoff of the S-IVB second burn. Using these variables, it is difficult to determine the magnitude of the in-plane and out-of-plane dispersions from the nominal state at translunar injection. Furthermore, it is desirable to determine the midcourse correction velocities required to compensate for errors in cutoff position and velocity magnitude, in-plane and out-of-plane angular errors, and out-of-plane position dispersions in the injection coordinate system.

Hypersurface Program This subsection outlines the purpose of the hypersurface concept and gives a brief description of the determination of the ellipse that is rotated to obtain what has come to be called the simplified hypersurface. A detailed description of the concepts behind the formulation of the hypersurface concept and a detailed description of how the hypersurface equations are implemented in the flight program will not be given here.

The basic function of the hypersurface equations is to provide out-of-orbit targeting cutoff conditions for the S-IVB second burn. These cutoff conditions are the terminal range, terminal

velocity, terminal flight path angle, and range angle and are used as initial inputs to the IGM. Used in conjunction with the hypersurface program is a navigation program for navigation in the parking orbit. This program is necessary to allow determination of the initiation of chill-down. The initial requirement toward describing out-of-orbit cutoff conditions is the determination of an aim vector $\vec{M}$. The aim vector lies along the earth-moon line (Figure 8) and represents the intersection of all possible flight conics that have the same terminal position at the moon. These conics have the same perilune magnitude, fixed flight time, and essentially constant energy. Targeting to a point ϵ is determined by the specification of an aim vector magnitude $|\vec{M}|$, the perigee half-cone angle σ and a representative energy C_3. The simplified hypersurface is formed by rotating this nominal conic about the aim vector $\vec{M}$ (Figure 9). The flight program operations that are necessary to obtain the cutoff conditions stated above are referenced.[2] These cutoff conditions are then used by IGM for optimal guidance of the second burn of the S-IVB to translunar injection. The nominal translunar injection state discussed in the above subsection on Midcourse Correction Program are simulated by first using the hypersurface and navigation programs and then using the 6D and IGM out-of-orbit programs.

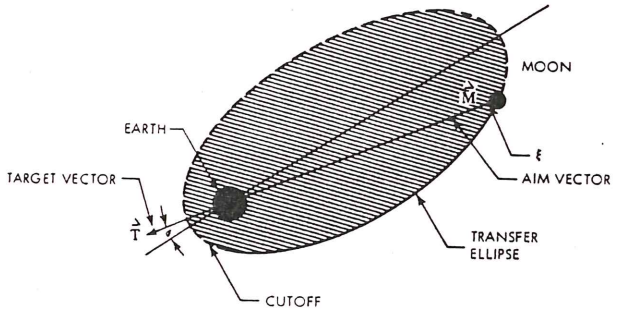

Figure 8. Geometry of Target Vector and Aim Vector

Properties of Midcourse Velocities

Injection Coordinate System Perturbations The purpose of this subsection is to describe the properties of the midcourse correction velocity required to compensate for in-plane and out-of-plane (injection orbit plane) perturbations in position and velocity at translunar injection. The nominal trajectory utilized in this analysis is

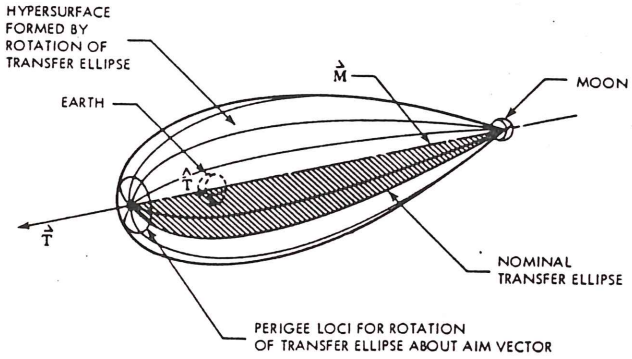

Figure 9. Geometry of the Simplified Hypersurface

described in Section II. The geometry which shows the perturbed quantities relative to the guidance reference system and the geometry between the geocentric inertial system and the injection coordinate system is depicted in Figures 10 and 11. (The geometry which describes the perturbed quantities relative to the guidance reference system and the geometry between geocentric inertial system and the injection coordinate system is also depicted in Figures 10 and 11.) The out-of-plane velocity perturbation ($\Delta\gamma y$) is given in terms of an out-of-plane flight path angle orthogonal to the injection orbit plane; whereas, the out-of-plane position perturbation (errors along the Z component of the injection coordinate system) is given in terms of a distance orthogonal to this same plane (Figures 10 and 11). The in-plane velocity flight path angle error is identified by $\Delta\gamma p$ (Figure A-1) while the errors in scalar position and velocity magnitude are given by ΔR and ΔV.

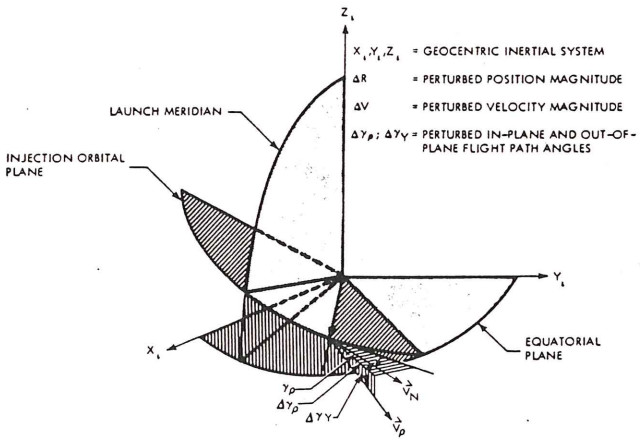

Figure 10. Geometry Between Geocentric Inertial System and Guidance Reference System and Velocity Perturbations

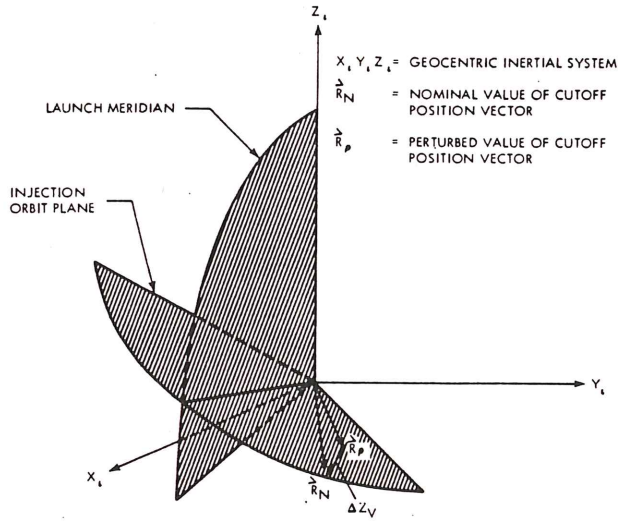

Figure 11. Geometry of In-Plane and Out-of-Plane Position Perturbation at Translunar Injection

The results of the in-plane and out-of-plane study are depicted in Figures 12 and 13. These figures and supporting tabular data show that:

- The out-of-plane velocity corrections are linear.
- The out-of-plane position magnitude errors require considerably less midcourse correction than do corresponding errors in the in-plane position magnitude.
- The out-of-plane error in flight path angle requires less midcourse correction than does a corresponding error in the in-plane flight path angle.
- The midcourse correction velocity for the out-of-plane position perturbation is symmetrical in velocity magnitude out to and including the fourth decimal place. Similar behavior, but with less agreement in magnitude symmetry, was observed in midcourse corrections for the in-plane position magnitude perturbations.
- For the out-of-plane velocity angle perturbations, the midcourse correction velocity magnitude deviates from symmetry beyond about one degree, with the larger correction being required for the negative perturbation. Similar behavior was noted for the in-plane velocity angular perturbation.

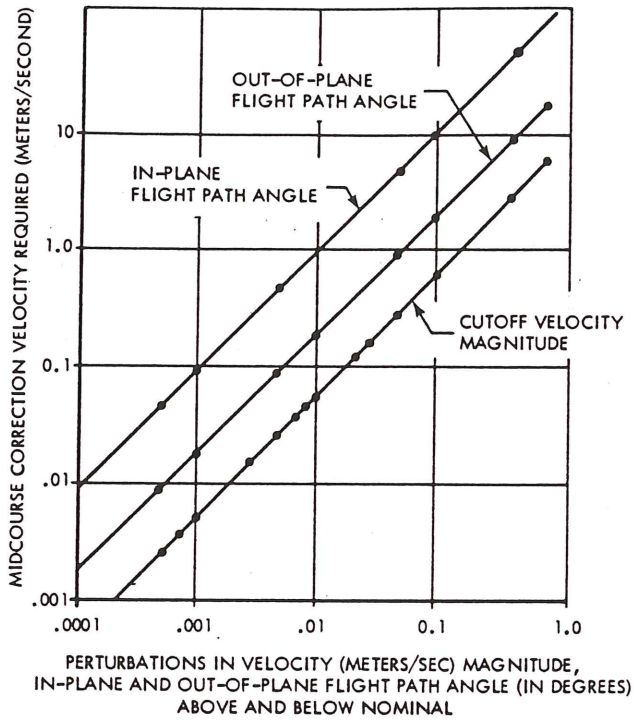

Figure 12. Midcourse Correction Velocity Magnitude as Function of Cutoff Velocity Magnitude, In-Plane and Out-of-Plane Cutoff Flight Path Angles

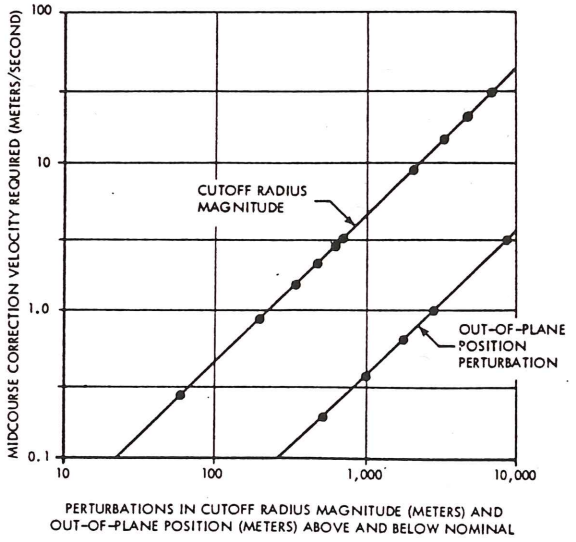

Figure 13. Midcourse Correction Velocity Magnitude as Function of Cutoff Radius Magnitude Perturbation and Out-of-Plane Position Perturbation

- The largest component of the velocity correction for both position and velocity perturbations is along the Z direction.

Geocentric Translunar Injection Perturbations

This subsection contains properties of the midcourse correction velocities and the relation of these velocities to the geocentric perturbations in position and velocity components at translunar injection. These position and velocity perturbations are depicted in Table 3-1.

Table 3-1

PERTURBATIONS AT TRANSLUNAR INJECTION IN GEOCENTRIC INERTIAL POSITION AND VELOCITY COMPONENTS

Row	Δ X(m)	Δ Y(m)	Δ Z(m)	Δ $\dot{X}$(m. sec)	Δ $\dot{Y}$(m. sec)	Δ $\dot{Z}$(m sec)
1	6,096.0	6,096.0	6,096.0	0.0	0.0	0.0
2	0.0	0.0	0.0	9.144	18.288	18.288
3	6,096.0	6,096.0	6,096.0	9.144	18.288	18.288
4	30.480	296.570	77.114	0.0	0.0	0.0
5	0.0	0.0	0.0	1.143	1.280	1.463
6	30.480	296.570	77.114	1.143	1.280	1.463
7	612.953	-53.340	1,102.157	0.0	0.0	0.0
8	0.0	0.0	0.0	1.378	2.725	-1.277
9	612.953	-53.340	1,102.157	1.378	2.725	-1.277
10	-20.117	9.449	25.969	0.0	0.0	0.0
11	0.0	0.0	0.0	0.045	-0.121	0.019
12	-20.117	9.449	25.969	0.045	-0.121	0.019
13	5,760.720	2,584.704	0.0	0.0	0.0	0.0
14	0.0	0.0	0.0	-8.047	0.0	29.017
15	5,760.720	2,584.704	0.0	-8.047	0.0	29.017
16	-4,206.240	-5,340.096	-21,689.568	0.0	0.0	0.0
17	0.0	0.0	0.0	-10.211	-30.450	-21.123
18	-4,206.240	-5,340.096	-21,689.568	-10.211	-30.450	-21.123
19	10,961.522	16,670.122	27,463.394	0.0	0.0	0.0
20	0.0	0.0	0.0	8.062	18.093	25.112
21	10,961.522	16,670.122	27,463.394	8.062	18.093	25.112
22	55,302.302	29,748.480	18,912.230	7.315	9.144	39.014
23	55,302.302	-29,748.480	18,912.230	7.315	-9.144	39.014
24	110,604.604	0.0	37,824.460	14.630	0.0	78.028

Approximate 3σ variations in the X, Y, and Z components are 3,048 meters (10,000 feet); while approximate 3σ variation in the X component of velocity is 4.57 m/sec (15 ft/sec) and in the Y and Z components is 9.14 m/sec (30 ft/sec).[2] The midcourse correction velocities for those perturbations in Table 3-1 are depicted in Table 3-2.

The information in Tables 3-1 and 3-2, and other perturbation and midcourse studies not described here, depicted the following behavior:

1. The magnitude of the components in one direction ($\Delta\dot{X}_{mc}$, $\Delta\dot{Y}_{mc}$, $\Delta\dot{Z}_{mc}$) of the midcourse correction velocities add

Table 3-2

MIDCOURSE CORRECTION VELOCITIES

Row	$\Delta\dot{X}_{mc}$(m/sec)	$\Delta\dot{Y}_{mc}$(m/sec)	$\Delta\dot{Z}_{mc}$(m/sec)	ΔV_{mc}(m/sec)
1	2.569	11.266	7.104	13.564
2	-33.633	-82.579	-45.665	100.180
3	-31.089	-71.267	-38.547	86.783
4	0.342	0.813	0.412	0.973
5	-3.473	-7.850	-4.342	9.620
6	-3.131	-7.038	-3.930	8.647
7	-.207	-.032	.390	.442
8	-3.891	-8.714	-4.485	10.545
9	-4.098	-8.746	-4.096	+10.491
10	+.052	.096	.060	.125
11	-.040	.016	.001	.043
12	.012	.112	.061	.128
13	-4.596	-4.637	-3.079	7.219
14	8.427	4.292	-.302	9.462
15	3.826	-.350	-3.383	5.119
16	-13.424	-31.813	-24.117	42.118
17	43.174	109.512	59.965	132.109
18	29.610	77.862	35.880	90.701
19	20.955	55.063	36.634	69.377
20	-33.258	-84.336	-47.250	102.231
21	-12.479	-29.063	-10.557	33.344
22	-65.725	-101.640	-57.236	+133.889
23	-116.032	-211.340	-107.475	263.967
24	-180.138	-313.114	-164.734	397.023

linearly to within truncation and round-off error of the programs used. For example, note that the first row of Table 3-1 contains perturbations in only the position components; whereas, the second row has perturbations in only velocity components. The third row has similar perturbations in both position and velocity. The first, second, and third rows of Table 3-2 give the magnitudes of the midcourse correction velocity components and the midcourse correction velocity for these cases. Note that the algebraic addition of the velocity components of the first two rows yields the third row to within the numerical error of the programs used to obtain these results.

2. The midcourse velocity magnitudes

$$\left|\Delta\vec{V}\right|_{mc} = \sqrt{(\Delta\dot{X}_{mc})^2 + (\Delta\dot{Y}_{mc})^2 + (\Delta\dot{Z}_{mc})^2}$$

do not add as scalars, but add as vectors. This result is also clear from physical reasoning. If the scalar properties held on the velocity magnitudes,

this would imply that velocity corrections being added would always be in the same direction regardless of the perturbations at injection. This property is illustrated by rows 13 through 15 of Tables 3-1 and 3-2. Note that the elements of rows 13 and 14 algebraically add to the velocity elements given in row 15 (to within the numerical errors in the program), while the velocity magnitudes do not scalarly add.

3. The magnitudes ($\Delta\dot{X}_{mc}$, $\Delta\dot{Y}_{mc}$, $\Delta\dot{Z}_{mc}$) of the components of the midcourse correction velocities are linearly related to the magnitudes of the respective ΔX, ΔY, ΔZ or $\Delta\dot{X}$, $\Delta\dot{Y}$, and $\Delta\dot{Z}$ perturbations at translunar injection provided that each of the components at translunar injection are increased by the same factor. For example, if the perturbations of row 10, Table 3-1, are increased by a factor of 10, the midcourse correction velocity components are increased by a factor of 10. If the components of velocity in row 8 are increased by a factor of 10, the resulting midcourse correction velocities required are increased by a factor of 10. Also, it may be shown that if each component of position and velocity is increased or decreased by the same factor, the midcourse correction velocity and velocity components are increased or decreased by the same factor. This conclusion, of course, is clear from the linearity of the functions.

Effect of Moon on Midcourse Correction Velocity

This analysis determines the effect of the moon on the midcourse correction velocity. The lunar trajectory with the moon not in the N-body model was obtained using the same initial conditions as those used to obtain the data in Table 3-2. The sensitivities for this trajectory were obtained and then used to obtain the midcourse correction velocities for those perturbations listed in Table 3-1. The results in Table 3-3a show that the effects of the moon on the magnitude of the midcourse correction velocity are negligible at the eight-hour point. However, as the midcourse correction point approaches the moon in time along the trajectory, these conditions change.

Table 3-3a

MIDCOURSE CORRECTION VELOCITY DIFFERENCES
(N-BODY WITH MOON OUT)

Row	Diff. $\Delta\dot{X}_{mc}$ (m/sec)	Diff. $\Delta\dot{Y}_{mc}$ (m/sec)	Diff. $\Delta\dot{Z}_{mc}$ (m/sec)	Diff. ΔV_{mc} (m/sec)
3	-0.0058	0.0043	0.0021	-0.0021
6	0.0006	0.0006	0.0	-0.0003
9	-0.0009	0.0003	0.0003	-0.0003
12	0.0	0.0	0.0	0.0
15	0.0015	0.0015	-0.0015	0.0021
18	0.0040	-0.0043	-0.0043	-0.0040
21	-0.0015	0.0018	0.0021	-0.0015
24	-0.0479	0.0125	0.0049	0.0098

Effect of Approximating N-Body Model (with Oblateness) with Two-Body Model

This analysis considers the accuracy of the midcourse correction velocities when using a two-body model rather than the N-body model to generate the trajectories. The trajectory and sensitivities were generated as described in the previous section. The resulting midcourse correction velocity differences are given in Table 3-3b for certain perturbations at translunar injection depicted in Table 3-1.

It can be seen that the model omitting the moon yields more accurate results than the two-body model, when compared with the N-body model. This is an expected result, since a spherical earth rather than an oblate earth was used. However, comparing the results of Tables 3-2 and 3-2b shows that the error in midcourse (correction velocity) is about one-tenth of one percent and is frequently less. Thus, one can conclude that the two-body model may be used unless exacting accuracy is required.

IV. Conclusions

The sensitivity and midcourse analyses have shown that the effects of the moon are negligible at the eight-hour midcourse correction point. It is also shown that the N-body model may be replaced with a two-body model in computing the midcourse correction velocities at the eight-hour point unless exacting accuracy is required. These results are depicted in Tables 3-3a and 3-3b. It was found that: (a) the midcourse velocity components in a given direction due to position and velocity errors, taken separately, yield the same result as when position and velocity errors are taken together and (b) the magnitudes of the components ($\Delta\dot{X}_{mc}$, $\Delta\dot{Y}_{mc}$, $\Delta\dot{Z}_{mc}$) of the midcourse velocity correction in a given direction are linearly related to the magnitudes of the position and velocity errors in that direction at translunar injection, provided each of the components is increased by the same amount. These results are given on pages 9 and 10 and in Tables 3-1 and 3-2.

The conclusions relating the midcourse velocities to errors in the injection coordinate system are given on pages 8 and 9, Figures 12 and 13. The primary conclusions are: (a) the magnitude of the midcourse correction velocity is linearly related to the individual errors in the in-plane and out-of-plane cutoff flight path angles, cutoff radius and velocity magnitude, and cutoff out-of-plane position dispersions, and (b) both the out-of-plane position and flight path angle errors require considerably less midcourse correction

Table 3-3b

MIDCOURSE CORRECTION VELOCITY DIFFERENCES
(N-BODY MINUS TWO-BODY)

Row	Diff. $\Delta\dot{X}_{mc}$ (m/sec)	Diff. $\Delta\dot{Y}_{mc}$ (m/sec)	Diff. $\Delta\dot{Z}_{mc}$ (m/sec)	Diff. ΔV_{mc} (m/sec)
3	0.1289	0.0116	0.0070	-0.0588
6	0.0128	0.0009	0.0009	-0.0061
9	0.0171	0.0034	-0.0018	-0.0088
12	-0.0001	0.0	0.0	0.0
15	-0.0165	-0.0140	0.0134	0.0204
18	-0.1177	-0.0180	0.0143	-0.0482
21	0.0475	0.0107	-0.0104	-0.0238
24	0.1926	0.1320	0.0695	-0.4977

than do the in-plane position magnitude error and the in-plane flight path angle error.

Appendix A. Translunar Injection Perturbation Equations Analysis

The purpose of this appendix is to briefly describe the formulation of the perturbation equations at translunar injection from which the perturbed trajectory states were obtained and the relation of this perturbed state to the geocentric inertial system. Both the in-plane and out-of-plane errors in the trajectory state are discussed.

The error equations for the position and velocity parametric studies are (see Figures A-1 and 11) as follows:

(1) Velocity

$$\Delta\dot{X}_V = \dot{X}_{VP} - \dot{X}_{VN}$$

$$= \left|\vec{V}_N + \Delta\vec{V}\right| \cos\Delta\gamma_y \cos$$

$$(\gamma_{PN} + \Delta\gamma_p) - \left|\vec{V}_N\right| \cos\gamma_{PN}$$

$$\Delta\dot{Y}_V = \dot{Y}_{VP} - \dot{Y}_{VN}$$

$$= \left|\vec{V}_N + \Delta\vec{V}\right| \cos\Delta\gamma_y \sin$$

$$(\gamma_{PN} + \Delta\gamma p) - \left|\vec{V}_N\right| \sin\gamma_{PN}$$

$$\Delta\dot{Z}_V = \dot{Z}_{VP} = \left|\vec{V}_N + \vec{V}\right| \sin\gamma_y$$

See definition of terms and Figure A-1.

(a) to determine $\left|\Delta\vec{V}\right|$ alone, set γ_y, $\Delta\gamma_p = 0$.

(b) to determine $\Delta\gamma_y$ alone, set $\left|\Delta\vec{V}\right|$, $\Delta\gamma_p = 0$.

If $\Delta\gamma_y$ [+; component of $\vec{V}_p$ in $+Z_V$ direction. / -; component of $\vec{V}_p$ in $-Z_V$ direction.]

(c) to determine $\Delta\gamma_p$ alone, set $\left|\Delta\vec{V}\right|$, $\Delta\gamma_y = 0$.

If $\Delta\gamma_p$ [+; greater than nominal value. / -; less than nominal value.]

(2) Position

The errors along the radius vector are given by $\Delta X_V = KX_{VN}$

$$\Delta Y_V = KY_{VN}$$

where K takes on positive and negative values. Note that the program computed $\Delta X_S = KX_S$, $\Delta Y_S = K\Delta Y_S$ and $\Delta Z_S = KZ_S$ where $X_S Y_S Z_S$ are the nominal values in the old plumb-line coordinate system. In the injection coordinate system there would be no perturbation of the position magnitude orthogonal to the translunar injection plane (as noted above). However, in the plumb-line coordinate system a component of $\vec{R}_n$ along Z exists because of geometrical orientation of the translunar injection plane to the plumb-line coordinate system.

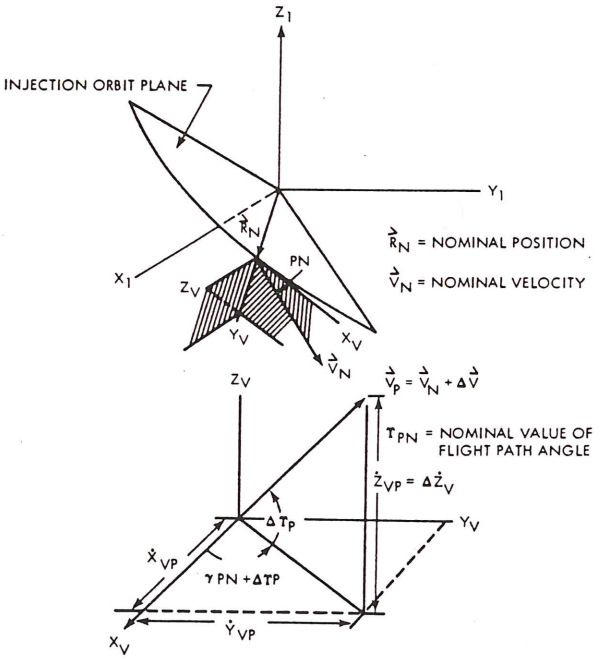

Figure A-1. Perturbation Geometry

The errors orthogonal to the injection orbit plane are given by

ΔZ_V (see Figure A-1) where

$$\Delta Z_V = KZ_{VN}$$

$$K = \begin{bmatrix} +; \text{ error along } + Z_V \text{ axis.} \\ -; \text{ error along } - Z_V \text{ axis.} \end{bmatrix}$$

The error components of position and velocity are transformed from the injection system to the inertial system using,

$$\begin{Bmatrix} \Delta X_I \\ \Delta Y_I \\ \Delta Z_I \end{Bmatrix} = \boxed{\begin{matrix} \text{TRANS} \\ \text{MATRIX} \end{matrix}} \begin{Bmatrix} \Delta X_V \\ \Delta Y_V \\ \Delta Z_V \end{Bmatrix}$$

$$\begin{Bmatrix} \Delta \dot{X}_I \\ \Delta \dot{Y}_I \\ \Delta \dot{Z}_I \end{Bmatrix} = \boxed{\begin{matrix} \text{TRANS} \\ \text{MATRIX} \end{matrix}} \begin{Bmatrix} \Delta \dot{X}_V \\ \Delta \dot{Y}_V \\ \Delta \dot{Z}_V \end{Bmatrix}$$

DEFINITION OF TERMS

γ_{PN} = Nominal value of in-plane flight path angle

$\Delta\gamma_P$ = Perturbed value of in-plane flight path angle

$\Delta\gamma_y$ = Perturbed value of out-of-plane flight path angle

$\vec{V}_N$ = Nominal value of cutoff velocity

$\Delta\vec{V}$ = Perturbed value of cutoff velocity

$\dot{X}_{VP}, \dot{Y}_{VP}, \dot{Z}_{VP}$ = Perturbed values of cutoff velocity in injection coordinate system

$\dot{X}_{VN}, \dot{Y}_{VN}, \dot{Z}_{VN}$ = Nominal values ot cutoff velocity in injection coordinate system

$\Delta\dot{X}_V, \Delta\dot{Y}_V, \Delta\dot{Z}_V$ = Errors from nominal velocity values in injection coordinate system

K = Assigned parameter value (tasks on both positive and negative values)

$\Delta X_V, \Delta Y_V, \Delta Z_V$ = Errors from nominal position values in injection coordinate system

X_{VN}, Y_{VN}, Z_{VN} = Nominal values of cutoff position in injection coordinate system

$|\vec{R}_P|$ = Perturbed value of position magnitude

$|\vec{R}_N|$ = Nominal value of position magnitude

Appendix B. Sensitivities Math Analysis

The purpose of this appendix is to give a brief description of the perturbation equations which, when integrated, will yield the perturbed geocentric inertial position and velocity components. The integration procedure is described in Hillsley's report.[4] These perturbed components, when added to the nominal position and velocity components, will yield, as a function of time, the perturbed trajectory state. The sensitivity matrix is used at the eight-hour midcourse correction state to obtain the perturbed trajectory state arising from the perturbed trajectory state at translunar injection.

The perturbation equations are developed as follows. The differential equation of motion of the vehicle in earth-moon space in the exterior of the lunar sphere of influence is given by Figure B-1.

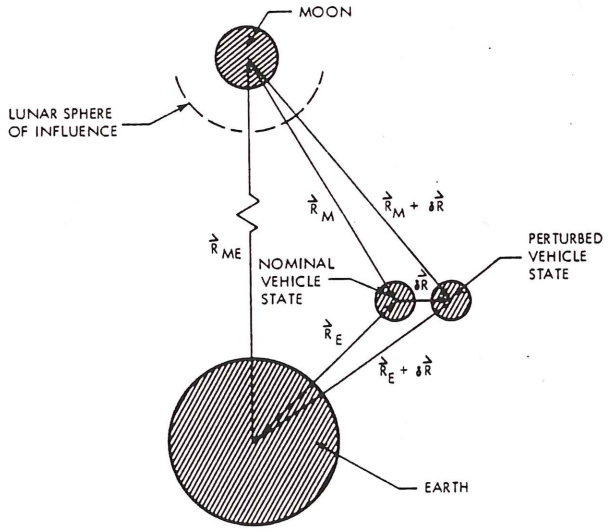

Figure B-1. Earth-Moon Geometry for Perturbation Equations (Not to Scale)

$$\ddot{\vec{R}}_E = \overbrace{-\frac{\mu_E \hat{R}_E}{R_E^3}}^{(a)} \overbrace{-\frac{\mu_M \hat{R}_M}{R_M^3}}^{(b)} \overbrace{-\frac{\mu_M \hat{R}_{ME}}{R_{ME}^3}}^{(c)} \quad (1)$$

where (a) = Force on vehicle due to the earth.
(b) = Force on vehicle due to the moon.
(c) = Force on earth due to moon. We consider this force because outside the lunar sphere of influence the earth is the primary attracting body.

The perturbation equation follows directly as

$$\delta\ddot{\vec{R}}_E = -\delta\left(\frac{\mu_E \hat{R}_E}{R_E^3}\right) - \delta\left(\frac{\mu_M \hat{R}_M}{R_M^3}\right) \quad (2)$$

The above equation becomes, when the indicated mathematical operations are performed,

$$\delta\ddot{\vec{R}}_E = A_E \delta\vec{R} + A_M \delta\vec{R}$$

where $\delta\ddot{\vec{R}}_E = \delta\ddot{\vec{R}}_M = \delta\ddot{\vec{R}}$ (3)

$$A_E = \frac{\mu_E}{R_E^5}\begin{Bmatrix} 3X_E^2 - R_E^2 & 3X_E Y_E & 3X_E Z_E \\ 3X_E Y_E & 3Y_E^2 - R_E^2 & 3X_E Y_E \\ 3X_E Z_E & 3Y_E Z_E & 3Z_E^2 - R_E^2 \end{Bmatrix}$$

$$A_M = \frac{\mu_M}{R_M^5}\begin{Bmatrix} 3X_M^2 - R_M^2 & 3X_M Y_M & 3X_M Z_M \\ 3X_M Y_M & 3X_M Y_M & 3X_M Z_M \\ 3X_M Z_M & 3Y_M Z_M & 3Z_M^2 - R_M^2 \end{Bmatrix}$$

Equation 3, when integrated by the methods described,[4] will yield the sensitivity matrix (which may be used to obtain the linear dispersions in state from the nominal trajectory) as a function of time.

References

1. MSC/MSFC Lunar Landing Reference Trajectory (U), Apollo Mission Planning Task Force Design Reference Mission, October 1965.

2. "Phase II Guidance Dynamics Recommendation Document for AS-504," IBM No. 67-228-0002, February 30, 1967.

3. "Translunar Injection Studies Step # 1 Report - IBM Programs for Translunar Trajectories," IBM No. 64-228-003H.

4. R. H. Hillsley, "Circumlunar Trajectory Sensitivities," IBM No. 66-512-007, August 21, 1964.

5. R. H. Battin, Astronautical Guidance (New York: McGraw-Hill Book Company, 1964) pp. 44-53.

6. Ibid., pp. 70-82.

Acknowledgments

Mr. Fred Bunnell provided the programming support in the translunar and transearth analysis and the sensitivity and midcourse correction velocity analysis. Mr. W. D. Riggs and Mr. Kyle Rone provided the simulation for the ascent-to-orbit, parking orbit, and translunar-injection phases.